

Pockels effect of water in the electric double layer at the interface between water and transparent electrode

Eiji Tokunaga^{a,*}, Yugo Nosaka^a, Masashi Hirabayashi^a, Takayoshi Kobayashi^{b,c}

^a Department of Physics, Faculty of Science, Tokyo University of Science, 1-3 Kagurazaka, Shinjyuku-ku, Tokyo 162-8601, Japan

^b Department of Applied Physics and Chemistry, and Institute for Laser Science, University of Electro-Communications, 1-5-1 Chofugaoka, Chofu, Tokyo 182-8585, Japan

^c Department of Electrophysics, Advanced Ultrafast Laser Center, National Chiao Tung University, 1001 Ta Hsueh Road, Hsinchu, 3005, Taiwan

Received 1 August 2006; accepted for publication 1 November 2006

Available online 20 November 2006

Abstract

We have obtained the first experimental evidence for the Pockels effect of water, which is induced by a high electric field in the electric double layer (EDL) on the water–transparent electrode interface. The electric-field induced energy shift of the visible interference fringes of a 300 nm indium–tin–oxide (ITO) electrode layer is observed, indicating a negative refractive index change at the interface. Numerical calculation reproduces well the experimental observation, showing that the signal mainly originates from water in the EDL. The Pockels constants of water are estimated to be $r_{33} = 5.1 \times 100$ pm/V and $r_{13} = 1.7 \times 100$ pm/V. The large anisotropy of the Pockels effect of water is deduced from the incidence angle dependence of the *p*-polarization signal. At the same time, the ITO shows a blue shift of the band gap in the UV due to the band population effect in the space charge layer. The plasma frequency in the near IR is also expected to increase due to the band population effect, since the ITO has a high doped carrier population close to metal. A negative refractive index change in the ITO space charge layer is induced from both effects, but its effect on the signal is estimated to be much smaller than that of the negative refractive index change of water in the EDL.

© 2006 Published by Elsevier B.V.

Keywords: Water; Pockels effect; Optical nonlinearity; Electric double layer; Indium oxides; Solid–liquid interfaces; Semiconducting surfaces; Metallic surfaces; ITO; Indium tin oxides; Refractive index; Electrolyte; Lock-in detection; Space charge layer; Transmission spectrum; Field effect; Visible/ultraviolet absorption spectroscopy; Non-linear optical methods; Interference

1. Introduction

Interaction between water molecules and biomolecules or solid surfaces turns water into new phases, different from bulk water. One of the most important is the electric double layer (EDL), which provides a field of various electrochemical reactions at the solid–aqueous solution interface. The thickness of the EDL is restricted to a nanometer scale, and it has been reported that water molecules have an orientational order in the EDL. As a result, the

static dielectric constant decreases to less than 10 from its bulk value of 80 [1–3]. This means that the orientational contribution to the polarizability is quenched while the vibrational and electronic contribution remains.

The orientational order of water molecules in the solid–liquid interface has been extensively studied both theoretically and experimentally [4,5]. The information on the molecular structure and molecular arrangement of interfacial water on various solid surfaces has been studied theoretically with various models [4] and experimentally by surface selective IR spectroscopy [5–9] as well as by surface X-ray scattering [10]. On the other hand, the optical properties, which reflect the electronic states, of water molecules on spatially restricted conditions are less understood than

* Corresponding author. Tel.: +81 3 5228 8214; fax: +81 3 5261 1023.
E-mail address: eiji@rs.kagu.tus.ac.jp (E. Tokunaga).

the structural properties of them because of the lack of experimental study.

The purely electronic response of such a highly ordered layer of water can be measured by the refractive index in the visible region. This is the Pockels effect of water, represented by the coefficient n_1 in the electric-field dependent refractive index $n = n_0 + n_1 E + n_2 E^2 + \dots$ or by the second-order susceptibility of $\chi_{ijk}^{(2)}(\omega; \omega, 0)$. A large number of study was devoted to the optical Kerr effect of water [11,12], expressed by the coefficient n_2 , or the third-order susceptibility of $\chi_{ijkl}^{(3)}(\omega; \omega, -\omega, \omega)$, because an intense electric field is readily applicable by using high-peak-power femtosecond optical pulses. In contrast, the Pockels effect of water has never been reported to the best of our knowledge. This is because the application of a high DC electric field is difficult due to the conductivity of water, and because bulk water has macroscopic centrosymmetry insensitive to the second-order nonlinear optical effects.

The electrolyte method for electroreflection spectroscopy [13,14] is a powerful tool for sensitively detecting the energy structure of doped semiconductors above the band gap and of metals. Even with an applied voltage as low as 1 V, a nanometer-scale electric double layer is formed at the water–semiconductor interface, where the voltage is concentrated. The space charge layer is then formed in the semiconductor surface due to the high electric field in the EDL. As a result, the carrier spatial and energy distribution function changes, which is accompanied by the reflectivity change. This is a kind of electrooptic effect, i.e., the Pockels effect, where the nonlinear refractive index change is proportional to the applied electric field. Although materials of a large electrooptic constant have been eagerly searched for from the requirement of optical information processing, the electrooptic constant involved in the electrolyte method has scarcely been evaluated. For most of the studies, furthermore, much attention has been paid to the refractive index change in the solid surface layer, but not in the EDL, with only a few exceptions [15,16]. Difficulty in evaluating the Pockels effect of water resides in the fact that the contribution of water to the refractive index change can hardly be separated from that of solid.

In this paper, we report the Pockels effect of water for the first time to the best of our knowledge. As an electrode for the electrolyte method, indium–tin–oxide (ITO) which is transparent in the visible is used. The applied voltage drops at the liquid–solid interface, i.e., in both the space charge layer of ITO and the electric double layer of electrolyte solution. The shift in the interference fringes of the thin ITO layer (nominally 300 nm) is detected in the transmission spectrum of the ITO in the electrolyte solution. The nonlinear refractive index change in the visible is readily evaluated from the shift. The contribution of the ITO to the signal is estimated from the spectral change in the UV absorption, where the band population effect induces the energy shift of the absorption edge. The result of analysis shows that most of the signal is caused by water in the EDL.

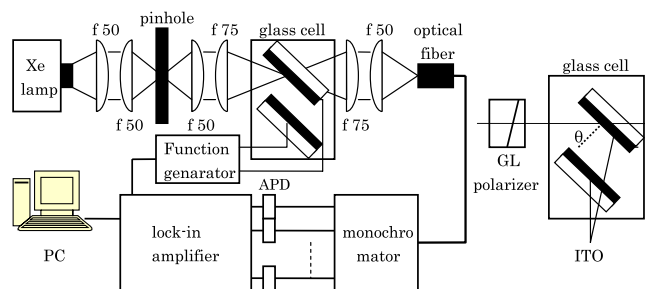


Fig. 1. Experimental setup. APD: avalanche photodiode. GL-polarizer: Glan-Laser polarizer. For lenses, the focal length of them are shown.

2. Experimental

We used electrodes made of ITO (Indium–Tin Oxide, Geomatec), where electrically conductive ITO thin films were formed by sputtering on glass substrates. The ITO is nearly transparent in the visible region. Its thickness, resistivity, and carrier density are 300 nm, $1.3 \times 10^{-4} \Omega \text{ cm}$, and $1.2 \times 10^{21} \text{ cm}^{-3}$, respectively. A typical experimental apparatus for electro-modulation measurement is shown in Fig. 1. A strong electrolyte solution, 0.1 M NaCl aqueous solution, was prepared from distilled water. Two ITO-electrodes were immersed in the solution filled in the glass cell. One electrode was grounded and AC voltage of 2 V (peak amplitude) was applied to the other at the frequency of $f = 20\text{--}500 \text{ Hz}$. A Xe lamp (Hamamatsu L2274) was used as a visible light source. The light from the lamp was incident into the glass cell and transmitted through the latter ITO electrode. The transmitted probe light was focused into a fiber-bundle input. The fiber bundle was connected to the input slit of a monochromator (Acton SP-308), and the laterally dispersed light by a grating (300 grooves/500 nm blaze) was received by 128 channel fiber bundle arrays at the exit of the monochromator. Each channel of the bundle fibers was connected to a Si avalanche photodiode (APD, Hamamatsu S5343). Photocurrents of 128 APDs were detected by a 128-channel lock-in amplifier [17,18]. The amplitude-modulated components of the APD photocurrents at the frequency of f were simultaneously measured as a function of channel number, each of which corresponds to a wavelength. This provides a difference transmission spectrum in the visible region induced by the first-order electrooptic (Pockels) effect. The probe light was made linearly-polarized by a Glan-Laser Polarizer, and the incidence angle dependence on the ITO for *s*- and *p*-polarization was investigated at the incidence angles of $\theta = 0^\circ$, 30° , and 45° . We tried also to measure the Kerr signal at $2f$ frequency, but detected a much smaller signal. Therefore, we limit our discussion on the f signal below.

3. Results

The thick solid curve in Fig. 2(a) shows the transmission spectrum of the ITO substrate. In the spectrum there are interference fringes which are due to the ITO layer of

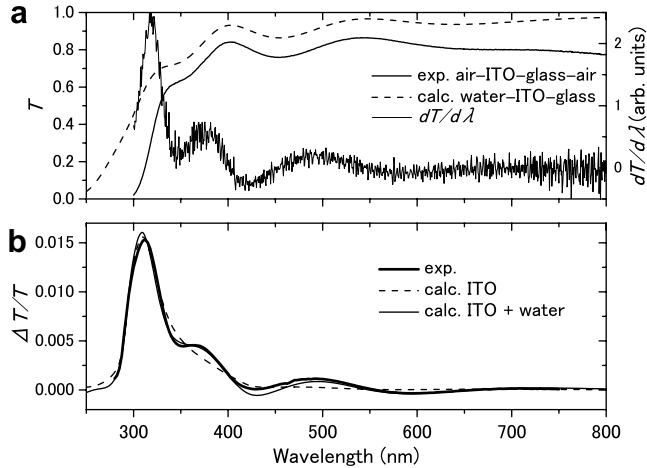


Fig. 2. (a) Measured and calculated transmission spectra. Thick solid curve measured for the 300-nm thick ITO-electrode on the glass substrate, placed in air. Dashed curve calculated for a 290-nm thick ITO placed between semi-infinite water and glass. Thin solid curve: the first derivative of the measured transmission spectrum of the ITO with respect to wavelength. (b) Measured and calculated difference transmission spectra normalized by the transmission spectrum. Thick solid curve measured at the normal incidence of the probe with $f = 40$ Hz, $V_{AC} = 2$ V, and $N_{NaCl} = 0.1$ M. Dashed curve calculated with the refractive index change only for the ITO. Thin solid curve calculated with the refractive index changes both for water in the EDL and for the ITO. For water, $\Delta n_0 = -0.1$ and $d_{EDL} = 2$ nm.

300 nm thickness. The transmission decrease in the UV region is due to the absorption edge of both ITO and glass substrate. The absorption edge of the ITO is blue-shifted from that of In_2O_3 due to the Burstein–Moss shift at the high level of Sn doping [19]. Similarly, there is a slight decrease in the transmission for the IR region, too. This is caused by metallic reflection due to the highly doped carrier density. The carrier density n of $1.2 \times 10^{21} \text{ cm}^{-3}$ gives the plasma frequency, $\sqrt{\frac{ne^2}{\epsilon_0 \epsilon_{opt} m_e}} / 2\pi$, of 2.8×10^{14} Hz, i.e., the high reflectivity for a longer wavelength than $1.08 \mu\text{m}$. Here, ϵ_0 is the permittivity of vacuum, ϵ_{opt} is the optical dielectric constant of the ITO, and m_e is the effective mass of carriers in the ITO given by $\epsilon_{opt} m_e = 1.24 m_0$, with m_0 being the electron mass [20].

Fig. 2(b) shows the normalized difference transmission spectrum $\Delta T/T$ due to the Pockels effect, where the probe light is normally incident. The thin solid curve in Fig. 2(a) is the first derivative of the transmission spectrum of the ITO film, indicating that the signal was caused by the refractive index change in the relevant layers, i.e., EDL or ITO. The blue shift of the interference fringes indicates a negative refractive index change. The top curves in Fig. 3 show the incidence angle dependence of the signals for s - and p -polarizations. In what follows, it is verified that the signal is caused by change in the refractive index of water in the EDL on the basis of a set of experiments and theoretical calculations.

Fig. 4 shows the signal intensity which depends on the electrolyte concentration and the modulation frequency. First, we varied the electrolyte (NaCl) concentration

between 0.0 M and 5 M as shown in Fig. 4(a). The thickness of the EDL (diffuse layer) is estimated as the Debye–Hückel length [21], which is given by

$$D = 0.304M^{-1/2}[\text{nm}]. \quad (1)$$

Here M is the electrolyte concentration (mol/l) [22]. Since the electric field strength in the EDL is inversely proportional to D for the same applied voltage, the signal intensity is expected to show the $M^{1/2}$ dependence if the optical non-linearity of water in the EDL is responsible for the signal. As seen in Fig. 4(a), the data are reasonably well fitted to a $M^{1/2}$ dependent curve. Second, we investigated the modulation frequency dependence of the $\Delta T/T$ signal as shown in Fig. 4(b). The signal intensity was found to increase with decreasing frequency. This result indicates that it takes time for the EDL to be completely formed responding to the applied electric field. The measured system consists of 0.1 M NaCl aqueous solution with two 0.4 cm-spaced ITO electrodes of 1 cm^2 size immersed. The standard impedance measurement shows that the equivalent circuit of the system consists of the solution resistance $R \sim 100 \Omega$ and the interface-layer (EDL and ITO) capacitance $C = 10\text{--}20 \mu\text{F}$. The experimental frequency dependence is explained by these circuit parameters; the voltage that falls on the interface layers increases with decreasing frequency. At 40 Hz, it is estimated that most (70–80%) of the applied voltage falls on the layers.

According to the above experimental observation, it is concluded that $\Delta T/T$ is caused by the formation of the EDL with a concentrated electric field as high as $\sim 10^9 \text{ V/m}$. The orientationally ordered H_2O molecules within the EDL is likely to be responsible for the refractive index change. However, one should also consider the effect of the induced high electric field on the ITO surface as well. On the surface, the space charge layer is formed by the band bending due to the high electric field. The signal in Fig. 2 shows that the net transmission increase (absorption decrease) in the UV region, which cannot be numerically reproduced by the refractive index change of water in the EDL only. Since the absorption edge of water lies in much higher energy region (above 200 nm) than in the measured wavelength region, the absorption change is attributed to the ITO electrode. The ITO sample is Sn doped In_2O_3 with carrier concentration of 10^{21} cm^{-3} . On the positive bias, both conduction and valence bands bend to the lower energy at the surface, increasing the carrier density in the space charge layer. The absorption edge then shifts to the higher energy due to the population increase in the conduction band. This is the field-induced Burstein–Moss shift, or the band population effect [23,24]. The blue shift of the absorption edge results in the net decrease in the absorption, inducing a negative refractive index change in the visible. In order to verify the Pockels effect of water, the contribution of the ITO to the observed interference-fringe shift must be estimated. In the next section, the experimental results are shown to be explained by the effect of water, not by that of ITO.

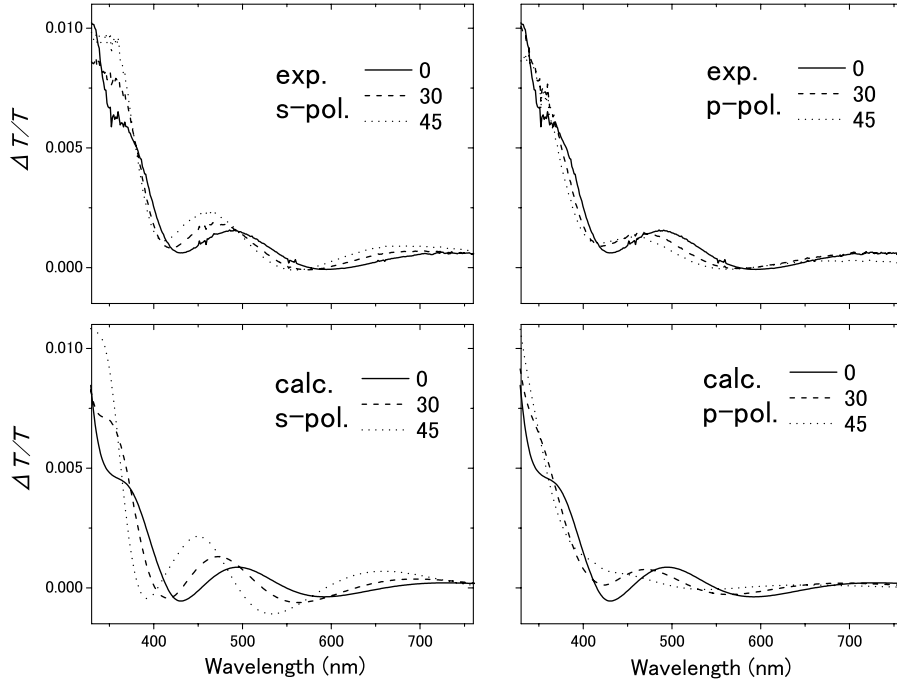


Fig. 3. Difference transmission spectra normalized by the transmission spectrum at each incidence angle. Top: experiments for *s*- and *p*-polarizations incident at $\theta = 0^\circ$, 30° , and 45° with $f = 40$ Hz, $V_{AC} = 2$ V, and $N_{NaCl} = 0.1$ M. Bottom: calculations with $\Delta n_o = -0.1$, $\Delta n_e = -0.3$, and $d_{EDL} = 2$ nm.

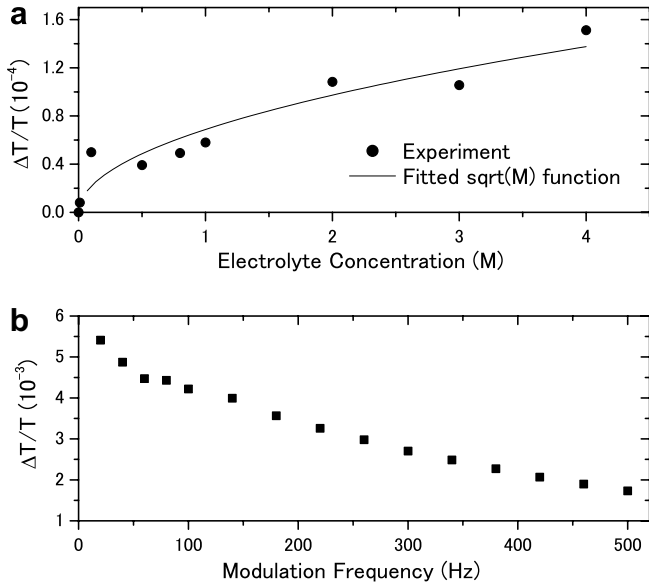


Fig. 4. (a) The electrolyte concentration dependence of the signal intensity with $f = 235$ Hz and $V_{AC} = 2$ V. (b) The modulation frequency dependence of the signal intensity at 468.3 nm with $V_{AC} = 2$ V and $N_{NaCl} = 0.1$ M.

4. Method of data analysis

In the present experiment, there are four dielectric layers involved; thick bulk water, ~ 1 nm EDL, 300 nm ITO, and thick glass substrate. In order to calculate the light transmission of multiply layered dielectric structure, we adopted the matrix method [25,26], where the EDL is approximated to be a constant-refractive-index layer. The parameter

values used are the refractive indices $n_w = 1.33$ for water, $n_{ITO} = n + ik$ for ITO as given in Fig. 5(a), $n_{glass} = 1.52$ for glass, and the layer thickness of $d_{ITO} = 290$ nm for ITO, and $d_{EDL} = 2$ nm for EDL. In order to treat the complex refractive index of the ITO layer properly in the method, the explicit expressions given in Ref. [26] are used. Here, the normal to the electrode surface is taken as the z -axis. The components of the refractive index ellipsoid of water without field is given by

$$x^2 + y^2 + z^2 = n_w^2. \quad (2)$$

Then it is distorted by the electric field F_z in the z -direction to make the refractive index ellipsoid [27,28]

$$\left(\frac{1}{n_w^2} + r_{13}F_z\right)(x^2 + y^2) + \left(\frac{1}{n_w^2} + r_{33}F_z\right)z^2 = 1. \quad (3)$$

The principal values of the refractive index, n_o and n_e , are related to the Pockels constants, r_{13} and r_{33} , respectively, as

$$n_o = n_w - \frac{1}{2}n_w^3 r_{13} F_z \quad (4)$$

and

$$n_e = n_w - \frac{1}{2}n_w^3 r_{33} F_z. \quad (5)$$

When the light beam is incident at the incidence angle θ , for *p*-polarization [29],

$$\frac{1}{n_p^2} = \frac{\sin^2 \alpha_p}{n_e^2} + \frac{\cos^2 \alpha_p}{n_o^2} \quad (6)$$

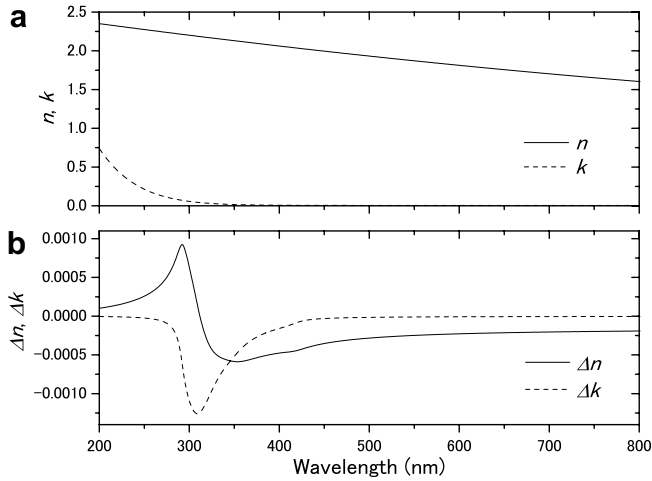


Fig. 5. (a) The complex refractive index (n_{ITO}) of the ITO assumed for the calculation of the dashed curve in Fig. 2(a). (b) The complex refractive index change (Δn_{ITO}) of the ITO assumed for the calculation of the dashed and thin solid curves in Fig. 2(b) and of the curves in the bottom of Fig. 3.

and for s -polarization,

$$n_s = n_o. \quad (7)$$

Here, α_p is the refracted angle in the EDL given by $n_w \sin \theta = n_p \sin \alpha_p$.

To fit the experimental transmission spectrum without the applied field (thick solid curve in Fig. 2(a)), the light transmission from bulk water through 290-nm ITO to bulk glass is considered. The calculated transmission spectrum is shown by the dashed curve in Fig. 2(a), where the assumed complex refractive index of the ITO is given in Fig. 5(a). The refractive indices of water and the glass are assumed to be $n_w = 1.33$ and $n_{\text{glass}} = 1.52$, respectively, and the UV absorption of the glass is not taken into account.

To fit the experimental difference transmission spectra in the UV region, the complex refractive index change in the ITO due to the band population effect is assumed to be given in Fig. 5(b). It is constructed from the optical susceptibility of multiple Lorentzians to satisfy the Kramers–Kronig relations. For simplicity, the thickness of the space charge layer of the ITO is not considered but the refractive index change is assumed to be uniform over the volume. This simplification does not cause serious errors. In fact, the calculated results are not much different even if the thickness is assumed to be 10 nm and correspondingly a larger refractive index change (as large as -0.01 at 400 nm) in the layer is assumed. The dashed curve in Fig. 2(b) shows the result calculated only with the complex refractive index change of ITO (without the refractive index change of water in the EDL). One can see the calculation reproduces the net transmission change in the UV region but it does not cause an appreciable shift in the interference fringes.

It is also expected that the band population effect increases the plasma frequency in the near IR to cause a considerable amount of the negative refractive index change in the visible, since the ITO has a high doped carrier popula-

tion close to that in metal. In order to estimate the contribution to the refractive index change of the band population effect (blue shift of both absorption edge and plasma frequency), the dielectric function in the space charge layer is assumed to be given as follows:

$$\frac{\varepsilon(\omega)}{\varepsilon_0} = \varepsilon_b + \frac{\omega_{p0}^2}{\omega_0^2 - \omega^2} - \frac{\omega_{p1}^2}{\omega^2}. \quad (8)$$

Here, ε_b is the background dielectric constant, ω_0 represents the absorption-edge energy, ω_{p0} is the plasma frequency for the density of bound electrons, and ω_{p1} is the plasma frequency for the doped free carriers. The damping constants are neglected without causing serious errors since the far off resonant change in the dielectric function in the visible is considered due to the change in the UV and IR region.

The band population effect changes the parameters as $\omega_0 \rightarrow \omega_0 + \Delta\omega_0$ and $\omega_{p1} \rightarrow \omega_{p1} + \Delta\omega_{p1}$. As a result,

$$\Delta \left(\frac{\varepsilon(\omega)}{\varepsilon_0} \right) = - \frac{2\omega_0 \omega_{p0}^2}{(\omega_0^2 - \omega^2)^2} \Delta\omega_0 - \frac{2\omega_{p1}^2}{\omega^2 \omega_{p1}} \Delta\omega_{p1}, \quad (9)$$

showing that positive values for $\Delta\omega_0$ and $\Delta\omega_{p1}$ gives a negative refractive index change. Using $\omega_p = \left(\frac{ne^2}{\varepsilon_0 m} \right)^{1/2}$ and $n = \frac{1}{3\pi^2} \left(\frac{2m\omega}{\hbar} \right)^{3/2}$ (density of carriers from the bottom of the conduction band up to $\hbar\omega$)

$$\frac{d\omega_p}{d\omega} = \frac{3m}{2\hbar} \left(\frac{e^2}{3\pi^2 \varepsilon_0 m} \right)^{2/3} \omega_p^{-1/3}. \quad (10)$$

For rough estimation, this equation gives $\Delta\omega_{p1} \sim 3\Delta\omega_0$ when $\omega_p = \omega_{p1}$ with $\hbar\omega_{p1} = 1$ eV, $\omega = \omega_0$, and m is the electron mass in vacuum. Substituting reasonable values for ω , ω_{p0} , and ω_{p1} in Eq. (9), both first and second terms in Eq. (9) give contributions of the same order of magnitude. The numerical calculation (dashed curve) in Fig. 2(b) shows that the blue shift of the absorption edge in the ITO ($\Delta\omega_0$ contribution) does not cause an appreciable fringe shift in the visible. The estimations from Eqs. (9) and (10) finally verify that the band population effect has a minor contribution to the observed interference-fringe shift in the visible, even if the plasma frequency change ($\Delta\omega_{p1}$ contribution) is included.

The thin solid curves in Fig. 2(b) and the curves in the bottom of Fig. 3 show the results of calculation with a negative refractive index change of water in the EDL added. The experimental spectra are reasonably reproduced both for s - and p -polarizations. Here, it is assumed that even without applied voltage, the EDL is formed due to a finite potential of zero charge (PZC) for ITO in 0.1 M NaCl such that the refractive index of water in the EDL is changed from that of bulk water as $n_o = n_w + 0.2$ and $n_e = n_w + 0.6$. To be precise, the 45° spectrum for p -polarization is not fitted very well compared with the other spectra. If the PZC is assumed to be zero, the fit becomes much worse for p -polarization.

The refractive index change of water which gives the best fit to the experiments is $\Delta n_o = -0.1$ and $\Delta n_e = -0.3$.

The parameter values used for the fit are $n_w = 1.33$, n_{ITO} and Δn_{ITO} given in Fig. 5, $n_{\text{glass}} = 1.52$, $d_{\text{ITO}} = 290$ nm, and $d_{\text{EDL}} = 2$ nm. To be consistent with $\Delta n_o = -0.1$ for +1 V, the voltage initially induced by surface charges in the ITO in 0.1 M NaCl solution must be -2 V, because it is assumed that $n_o = n_w + 0.2$.

Finally we obtained the Pockels constants of water from Eqs. (4) and (5) as

$$r_{33} = 5.1 \times 100 \text{ pm/V} \text{ and } r_{13} = 1.7 \times 100 \text{ pm/V.}$$

Here, the local field is not considered and the applied voltage of 2 V is assumed to be equally divided into the two EDLs in average. This assumption is justified because the signals for both ITO electrodes, i.e., for the grounded electrode and for the voltage-applied electrode, have exactly the same magnitude but have the opposite sign to each other. This result indicates that the applied voltage is symmetrically divided into two electrodes. More precisely, the temporal change of the sinusoidal electric fields that the two electrodes feel are the same except for the phase difference of π . In fact, the applied voltage falls partly on the ITO space charge layer and the bulk solution, so that these values are minimum estimates. These values are much larger than those for the well known electrooptic crystal LiNbO₃ [27,28]: $r_{33} = 30.8$ pm/V and $r_{13} = 8.6$ pm/V.

5. Discussion

Bulk water without interface does not have the second-order nonlinearity, or first-order electrooptic effect, because the dipole moments of water molecules are randomly distributed to have macroscopic centrosymmetry. The presence of the electrode interface, which breaks centrosymmetry, is essential for the Pockels effect of water. The microscopic origin of the Pockels effect of water possibly comes from the following effects:

(1) *Orientation of water molecules*: It is not known how water molecules are arranged at the bulk–water/ITO interface, but it is most likely that the dipole moments of water molecules at the compact layer are oriented depending on the polarity of the electrode, as reported for the Ag(111) interface [10] for example. The anisotropic nonlinear refractive index change must be caused by the DC-electric-field induced orientation change of water molecules at the electrode interface. The normal to the electrode surface (z -axis) is the principal axis of the refractive index ellipsoid. Considering $n_w = 1.33$, $\Delta n_o = -0.1$ and $\Delta n_e = -0.3$ gives large anisotropy. The principal polarizability of the water molecule has been reported to be nearly isotropic both experimentally [30] and theoretically [31]. The observed anisotropy is not consistent even with an anisotropic polarizability model [32,33]. It is therefore difficult to explain the large anisotropy of the ellipsoid solely from the molecular alignment.

(2) *Deformation or compression of water molecules*: In order to explain the anisotropy, effects other than molecular orientation might be considered such as molecular

deformation or the interaction with the atoms at the electrode surface. Firstly, there are theoretical studies to report that water molecules are compressed at the electrode surface resulting in the increase in the refractive index of water [15,16]. In fact, it was experimentally observed that water molecules are compressed to have an increased areal density at the Ag(111) interface [10]. Along the line of molecular compression, the result can be explained as follows: The ITO surface is initially charged at the zero external field due to a finite PZC, as assumed in the simulation in Fig. 3. Consequently, water molecules in the EDL are compressed to have a larger refractive index than that in bulk. By application of positive voltage, the refractive index recovers to that of bulk as the flat band condition is approached. The initial surface charge must be negative, as expected for ITO which is a negatively-doped large-bandgap semiconductor. Secondly, there is an experimental report on the structure of water monolayers at RuO₂/bulk water interface in Ref. [34], where water molecules interact with oxygen atom of RuO₂. In this case the interfacial monolayer would be subject to a large refractive index change. However, it is questioned whether a large change extends to 2 nm, as assumed in the present calculation.

(3) *Effect of electrolyte concentration*: When the EDL is formed at zero external field, ionic concentration at the layer is much higher than in bulk, leading to a higher refractive index of electrolyte solution than that of pure water. However, even for saturated NaCl solution (5.4 M, 26.4 wt% at 20 °C), the refractive index is 1.38. The observed large refractive index change and anisotropy could not be explained in terms of the ionic intensity.

(4) *Adsorption of anions*: Large radius anions such as chlorine and iodine ions are known to be adsorbed at the metal surface, which might affect the refractive index at the interface. However, we examined 0.1 M NaF solution also and obtained as large a signal as NaCl solution. Since fluorine ions are not adsorptive, the effect of adsorption is excluded.

Presently, we cannot identify the microscopic origin of the Pockels effect of water. The effects (1) and (2) are most likely, but they do not provide the complete solution. In order to explain both magnitude and anisotropy of the nonlinear refractive index change of water, the deformation of the molecular structure, the interaction with the atoms at the electrode surface [34], the intermolecular interaction between water molecules, and cooperative effects in the hydrogen-bond network of water [33,35–38] are all to be fully considered.

6. Summary

The Pockels effect of water in the electric double layer was observed for the first time. The anisotropic, large refractive index change of water is induced in the nanometer-scale electric double layer at the interface between water and transparent electrode (ITO, In₂O₃ doped with SnO₂).

The Pockels constants of water for 0.1 M NaCl aqueous solution were estimated to be more than ten times larger than those for the standard electrooptic crystal, LiNbO₃. The response time of the effect is an order of 0.001 s (RC time const) because it is limited by the formation time of the electric double layer. The band population effect of ITO was also observed for the first time, but it is estimated to have a little effect on the observed shift of the interference fringes.

There are still several problems left to be solved. First, the incidence-angle dependence of the difference transmission spectra for both s - and p -polarizations is reasonably well fitted with the calculation. To be precise, however, the fit is not perfect especially at 45° incidence for p -polarization, where there is appreciable qualitative difference. Second, we assumed the potential of zero charge (PZC) of ITO in the experimental condition is 2 V, but it must be precisely evaluated. Third, the thickness of the space charge layer of ITO is taken to be more than 10 nm, but if it is an order of 1 nm, the calculation shows that the complex refractive index change of ITO has an appreciable effect on the shift of the interference fringes. Fourth, the applied voltage is actually divided into both the EDL and the space charge layer of ITO, but the division ratio is not evaluated at present. One must also clarify whether the Pockels effect of water depends on the character of the interface, i.e., on the electrode materials such as oxides, metals, and semiconductors. In order to finally fix the values for the Pockels constants of water, these problems are to be solved.

Acknowledgements

The authors thank Geomatec Co. Ltd. for supplying the ITO substrates and Takahiro Shijo for his experimental help at the initial stage of the research. This research is supported by the Promotion and Mutual Aid Corporation for Private Schools of Japan and by Research Center for Green Photo-Science and Technology to E.T. and also by the Grant-in-Aid for Specially Promoted Research (#14002003) from the Ministry of Education, Culture, Sports, Science and Technology and by International Cooperative Research Project (ICORP), Japan Science and Technology Agency to T.K.

References

- [1] G.E. Brown Jr., V.E. Henrich, W.H. Casey, D.L. Clark, C. Eggleston, A. Felmy, D.W. Goodman, M. Gratzel, G. Maciel, M.I. McCarthy, K.H. Neelson, D.A. Sverjensky, M.F. Toney, J.M. Zachara, *Chem. Rev.* 99 (1999) 77.
- [2] F. Booth, *J. Chem. Phys.* 19 (1951) 391.
- [3] I. Danielewicz-Ferchmin, A.R. Ferchmin, *Phys. Chem. Chem. Phys.* 6 (2004) 1332.
- [4] J. Sobkowski, M. Jurkiewicz-Herbich, in: J.O'M. Bockris, R.E. White, B.E. Conway (Eds.), *Modern Aspects of Electrochemistry*, vol. 31, Plenum, New York, 1997, p. 1.
- [5] I. Benjamin, in: J.O'M. Bockris, R.E. White, B.E. Conway (Eds.), *Modern Aspects of Electrochemistry*, vol. 31, Plenum, New York, 1997, p. 115.
- [6] Q. Du, E. Freysz, Y.R. Shen, *Phys. Rev. Lett.* 72 (1994) 238.
- [7] K.A. Becraft, G.L. Richmond, *Langmuir* 17 (2001) 7721.
- [8] K. Ataka, T. Yotsuyanagi, M. Osawa, *J. Phys. Chem.* 100 (1996) 10664.
- [9] S. Nihonyanagi, S. Ye, K. Uosaki, L. Dreesen, C. Humbert, P. Thiry, A. Peremans, *Surf. Sci.* 573 (2004) 11.
- [10] M.F. Toney, J.N. Howard, J. Richer, G.L. Borges, J.G. Gordon, O.R. Melroy, D.G. Wiesler, D. Yee, L.B. Sorensen, *Surf. Sci.* 335 (1995) 326.
- [11] P.P. Ho, R.R. Alfano, *Phys. Rev. A* 20 (1979) 2170.
- [12] R. Torre, P. Bartolini, R. Righini, *Nature* 428 (2004) 296.
- [13] R. Williams, *Phys. Rev.* 117 (1960) 1487.
- [14] K.L. Shaklee, F.H. Pollak, M. Cardona, *Phys. Rev. Lett.* 15 (1965) 883.
- [15] G.J. Hills, R. Payne, *Trans. Faraday Soc.* 61 (1965) 326.
- [16] M. Stedman, *Chem. Phys. Lett.* 2 (1968) 457.
- [17] N. Ishii, E. Tokunaga, S. Adachi, T. Kimura, H. Matsuda, T. Kobayashi, *Phys. Rev. A* 70 (2004) 023811.
- [18] T. Ogawa, E. Tokunaga, T. Kobayashi, *Chem. Phys. Lett.* 408 (2005) 186.
- [19] I. Hamberg, C.G. Granqvist, *Phys. Rev. B* 30 (1984) 3240.
- [20] Y. Ohhata, F. Shinoki, S. Yoshida, *Thin Solid Films* 59 (1979) 255.
- [21] D.C. Grahame, *Chem. Rev.* 41 (1947) 441.
- [22] T. Watanabe, K. Kanemura, H. Masuda, M. Watanabe, *Electrochemistry*, Maruzen, Tokyo, 2001 (in Japanese).
- [23] R. Glosser, B.O. Seraphin, *Phys. Rev.* 187 (1969) 1021.
- [24] N. Bottka, D.L. Johnson, R. Glosser, *Phys. Rev. B* 15 (1977) 2184.
- [25] M. Born, E. Wolf, *Principles of Optics*, sixth ed., Pergamon Press, Oxford, 1980.
- [26] M. Kobiyama, *Theory of optical thin films*, second ed., Optronics, Tokyo, 2003 (in Japanese).
- [27] R.W. Boyd, *Nonlinear Optics*, Academic Press, New York, 1992.
- [28] A. Yariv, *Quantum Electronics*, third ed., Wiley, New York, 1988.
- [29] C.C. Teng, H.T. Man, *Appl. Phys. Lett.* 56 (1990) 1734.
- [30] W.F. Murphy, *J. Chem. Phys.* 67 (1977) 5877.
- [31] G. Maroulis, *J. Chem. Phys.* 94 (1991) 1182.
- [32] C. Huiszoon, *Mol. Phys.* 58 (1986) 865.
- [33] W.B. Bosma, L.E. Fried, S. Mukamel, *J. Chem. Phys.* 98 (1993) 4413.
- [34] Y.S. Chu, T.E. Lister, W.G. Cullen, H. You, Z. Nagy, *Phys. Rev. Lett.* 86 (2001) 3364.
- [35] I. Ohmine, S. Saito, *Acc. Chem. Res.* 32 (1999) 741.
- [36] Y. Tominaga, A. Fujiwara, Y. Amo, *Fluid Phase Equilibria* 144 (1998) 323.
- [37] E.W. Castner Jr., Y.J. Chang, Y.C. Chu, G.E. Walrafen, *J. Chem. Phys.* 102 (1995) 653.
- [38] K. Winkler, J. Lindner, H. Bürsing, P. Vöhringer, *J. Chem. Phys.* 113 (2000) 4674.